

Quantum Conductance in Silver Nanowires: correlation between atomic structure and transport properties

V. Rodrigues^{1,2}, J. Bettini¹, A.R. Rocha^{1,2}, L.G.C. Rego¹, and D. Ugarte^{1*}

¹*Laboratório Nacional de Luz Síncrotron,*

C.P. 6192, 13084-971 Campinas SP, Brazil and

²*Instituto de Física "Gleb Wataghin", UNICAMP,*

C.P. 6165, 13083-970 Campinas SP, Brazil

(Dated: November 5, 2018)

Abstract

We have analyzed the atomic arrangements and quantum conductance of silver nanowires generated by mechanical elongation. The surface properties of Ag induce unexpected structural properties, as for example, predominance of high aspect ratio rod-like wires. The structural behavior was used to understand the Ag quantum conductance data and the proposed correlation was confirmed by means of theoretical calculations. These results emphasize that the conductance of metal point contacts is determined by the preferred atomic structures and, that atomistic descriptions are essential to interpret the quantum transport behavior of metal nanostructures.

PACS numbers: 68.65.+g, 61.16.Bg, 73.50.-h

The physical interpretation of the presence of flat plateaus and abrupt jumps on the electrical conductance of metal nanowires (NWs) [1] has been controversial, because its discrete nature has been either attributed to electron channels [2, 3] or to structural rearrangements [4]. Since the beginning of this research field, the basic experiment for studying the NW conductance has been based on the elongation of junctions or point contacts [5], while measuring their electrical properties. In fact, it has been extremely difficult to discriminate between structural and electronic effects in a NW elongation experiment, because both are simultaneously modified during the measurement [6].

Recently, the application of time-resolved High Resolution Transmission Electron Microscopy (HRTEM) in the study of gold NWs has revealed the existence of suspended atom chains (ATCs), whose conductance was measured to be equal to the universal quantum, $G_0 = 2e^2/h$ (where e is the electron charge and h is Planck's constant) [7]. Subsequently, a broader correlation between atomic structure and conductance has been derived for Au NWs [8] where a simple extension of the Wulff construction [9] was used to predict the NW morphologies based on the crystallographic directions. For example, it is well-known that the Au compact (111) facets are preferred and, then, nanosystems evolve to expose mainly these low energy facets [9].

Although significant progress has been done to understand NW properties, most of the reported studies are actually based on gold (see recent review in [1]). Moreover, the majority of the available evidence is derived indirectly on the basis of average statistical behaviors [3, 8]. To get a deeper and more general insight it is necessary to analyze still other model systems, as for example, different monovalent metals (to easily describe the conductance) and, if possible, with different surface properties (in order to induce different NW structures). Silver represents an excellent point in case, because it is a face centered cubic (fcc) metal with a lattice parameter similar to that of gold, nonetheless, the silver minimal energy facets are (100) oriented [10]. It must be emphasized, that the higher reactivity of silver has hindered detailed studies of quantum conductance (QC) in such system [11].

In this work, we have used two independent experimental methods to analyze silver NW structures and their conductance, finding that the observed Ag NW properties differ strongly from the previously studied systems. Theoretical predictions have been used to consistently correlate the structural and QC behavior. The results provide new information to understand the conductance properties of nanosystems.

We have generated the silver NWs *in situ* in a HRTEM using the procedure reported by Kondo and Takayanagi [12], who were able to produce NWs by making holes in a metal self-supported thin film. The silver film was polycrystalline (5 nm thick, average grain size 50-100 nm); a detailed description of this experimental procedure was given previously [8, 13]. The HRTEM observations were performed using a JEM 3010 URP with a 0.17 nm point resolution (LME/Lab. Nac. Luz Síncrotron, Campinas, Brazil). All imaging work was acquired close to Scherzer defocus [14], and the presented images were generated by the digitalization of video recordings (30 frames/s) acquired using a high sensitivity TV Camera (Gatan 622SC). This kind of *in situ* HRTEM NW study has been previously performed with high efficiency on gold and platinum [7, 8, 12, 13, 15, 16, 17, 18]. However, silver NWs have been much more difficult to image with similar quality. Firstly, due to the lower atomic number the generated contrast is much weaker; secondly, Ag NWs display a much faster evolution, rendering difficult the real time image acquisition.

The electrical conductance of silver NWs was measured with an independent and dedicated instrument: a Mechanically Controllable Break Junction (MCBJ) [19] operating in ultra-high-vacuum (UHV) [20] ($< 10^{-8}$ Pa). In this method, a silver wire ($\phi = 75 \mu\text{m}$, 99.99 % pure) is broken *in situ* in UHV and NWs are generated by putting into contact and subsequently retracting these clean surfaces. The electronics is basically composed of a home-made voltage source and a current-voltage converter coupled to an 8 bits digital oscilloscope (Tektronic TDS540C). The acquisition system input impedance and time response were optimized to perform conductance measurements in the [0-4] G_0 range with a relative error of $\Delta G/G \sim 10^{-4}$.

The time-resolved HRTEM observations of silver NWs have revealed some striking and unexpected structural behavior, which contrast strongly with the results reported for gold [7, 8, 12, 13, 17]. In particular, high aspect-ratio rod-like NWs along the [110] direction (hereafter noted as [110] NW) are the most frequently observed morphology. As an example, in Fig. 1, we show a series of snapshots of a complete elongation/thinning process of a pillar shaped NW. Initially, the rod is formed by 5 (200) atomic planes (thickness ~ 0.8 nm, Fig. 1a), losing sequentially one atomic plane at a time to attain a three layer thickness (~ 0.4 nm, Fig. 1c). Subsequently in Fig. 1d, the right side of the wire becomes thicker, while the left side maintains the same width (~ 0.4 nm) as in Fig. 1c. However, this left sector shows a quite different contrast pattern, the HRTEM image shows darker dots for

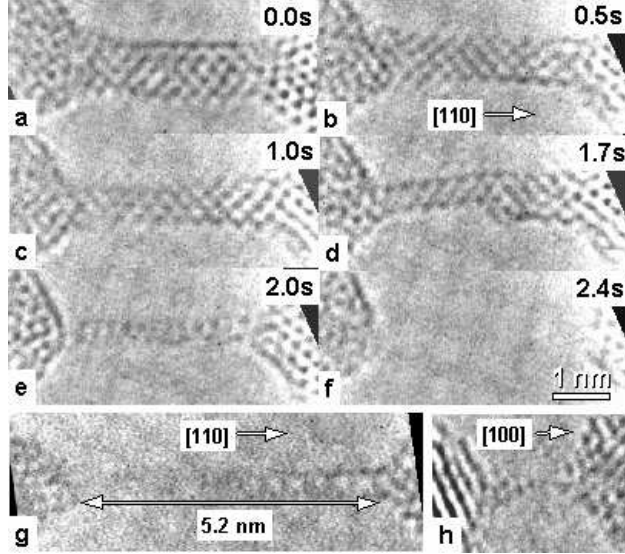


FIG. 1: a-f) Atomic resolution micrographs showing the elongation and thinning of a rod-like silver nanowire (see text for explanations); g) HRTEM image of a high aspect-ratio pillar like NW (width ~ 0.4 nm and length is ~ 5 nm); h) HRTEM micrograph of silver suspended atom chain. Atomic positions appear dark.

the external planes (tube-like), whereas the central layer contrast is much weaker. Finally, before breaking, the minimal observed size for this morphology consists of two (200) atomic planes (~ 0.2 nm wide, Fig. 1e). All the lattice fringes and angular relations observed in the HRTEM images of Ag NWs can be fully described by means of the bulk silver fcc structure. It is important to note that NWs showing the tube-like contrast pattern are frequently observed in the experiments and the underlying atomic structure seems to be particularly stable because they can attain aspect-ratios > 10 (see example in Fig. 1g). In addition, the final length of these tube-like NWs is not determined by the initial size, as evidenced in Fig. 1a-f. In fact, in many cases, we have observed that when the wire attains this peculiar structure (or contrast pattern), the apexes retraction cause the NW to elongate by a factor $\sim 1.5-3$ without thinning. This lengthening reflects the enhanced strength of this atomic configuration.

As for the existence of silver suspended atom chains, our results confirm that they do occur, nevertheless they are much less frequently observed than in our previous studies of gold and platinum NWs [8, 13, 17, 18]. In fact, they are only seen when one of the junction apexes is oriented along a [100] direction. These ATCs are 2-4 atoms long with a

bond length in the 0.33-0.36 nm range. Both the lengths and bond distances are similar to previous reports on Au and Pt ATCs [7, 8, 17, 18, 21]. However an important difference has been revealed by the dynamic HRTEM recordings, which have pointed out that silver [111] NWs display a fast and abrupt rupture preventing the formation of ATCs (within our time resolution).

In order to deduce the three dimensional atomic arrangement of the nanowire from the HRTEM images (basically a bidimensional projection), the geometrical Wulff construction [9] can be used. This approach yields the crystal shape by predicting the relative size of the lower energy facets of the crystal. Recently, it has been successfully applied to describe and model gold nanojunctions [8]. Fig. 2 shows the application of the Wulff method to model the morphology of silver rod-like NWs. It is instructive to look first at the expected morphology of a silver nanoparticle, a truncated cuboctahedron with regular triangular (111) facets, where the relevance of (100) facets can be easily identified (see Fig. 2a)[22]. The cross section of a [110] silver NW can be derived by looking at this cuboctahedron along the [110] axis. Figs. 2b and 2c show the suggested cross-sections for the rod-like NWs seen in Figs. 1a and 1c, which are formed by 5 and 3 (200) atomic planes, respectively. These rods are generated by the alternate stacking of two different planes containing 11 and 8 atoms (marked 11/8, and displayed with different colors in Fig. 2b) for the thicker NW and 4/3 atoms for the thinner one (Fig. 2c). When these rods are observed along a [1-10] axis (as in the experiment), we observe the bidimensional projection indicated as side views in Fig. 2. In a first approximation, at the Scherzer defocus [14] and for such a thin object, the expected contrast at each atomic column position should be proportional to the projected atomic potential or, in other words, the number of atoms along the observation direction. In Fig. 1d, the NW contrast is tube-like, with the external planes much darker than the central one. Thus, on the light of the preceding argument, the central atomic columns should contain less atoms than the border ones. The only way to fulfill these conditions, by thinning the 4/3 rod (Fig. 2c), is to build a 4/1 NW (see Fig. 2d). Finally, the thinnest Ag [110] NW, shown in Fig. 1e, consists of two atomic planes. Two atomic arrangements may yield the observed contrast: a 2/1 structure with a triangular cross-section (Fig. 2e), or two parallel atom chains marked as 1/1 in Fig. 2f. The signal-to-noise ratio in the image does not allow us to identify which one is observed in Fig. 1e. Recently, Hong *et al* [23] have reported the preparation of Ag [110] rod-like NWs within porous matrix by means of

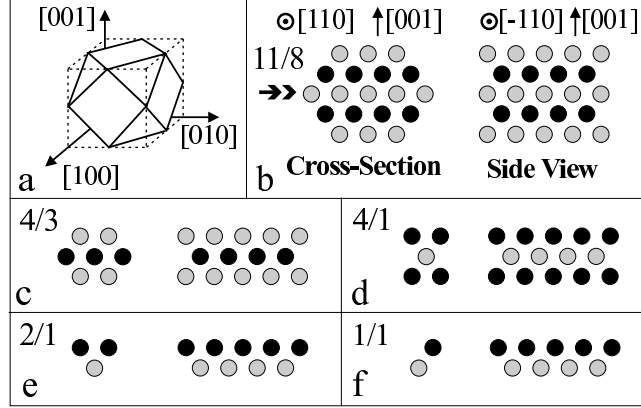


FIG. 2: a) Application of the Wulff construction [9] to determine the shape of silver nanoparticles. b-f) Scheme of possible atomic arrangements for rod-like Ag NWs; we show the NW cross-sections and also, side views (observed along the horizontal arrow in b).

wet chemical methods. However the generated structure (which can be described as 2/2 following our notation) has not been observed in the free standing Ag NWs studied here.

The discussion presented above allows the deduction of the atomic structures for the NW morphology that have been most frequently observed during the HRTEM studies. It is now tempting to correlate the preferred atomic arrangements with the quantum conductance properties. Fig. 3 shows typical conductance curves of Ag NWs (see inset) and, a histogram of occurrence of each conductance value (global histogram [1]) obtained from 500 conductance curves. This histogram shows large peaks at $1 G_0$, $\sim 2.4 G_0$ and $\sim 4 G_0$. It also displays major differences when compared to similar results reported for gold NWs [1]. In the first place, the $1 G_0$ peak is not the dominant one [1, 8], in accordance with the HRTEM data that shows low occurrence of atom chains. Secondly, the absence of the $2 G_0$ peak (usually located at $\sim 1.8 G_0$ in Au histograms [1]) evidences that the structure of silver NWs should be much different. In addition, the large peak at $2.4 G_0$ displays an area approximately 2.5 times bigger than the peak close to $1 G_0$. This fact suggests that this conductance is associated with a more frequently occurring structure, which has to be identified as the rod-like [110] NWs observed in our HRTEM experiments. Because the minimal observed [110] Ag NW should consist of two atomic layers (Fig. 2e), it is tempting to associate the conductance peak at $\sim 2.4 G_0$ with this structure.

Finally, to consistently correlate the experimental results of the conductance and structural behaviors, we have performed theoretical conductance calculations for the structures

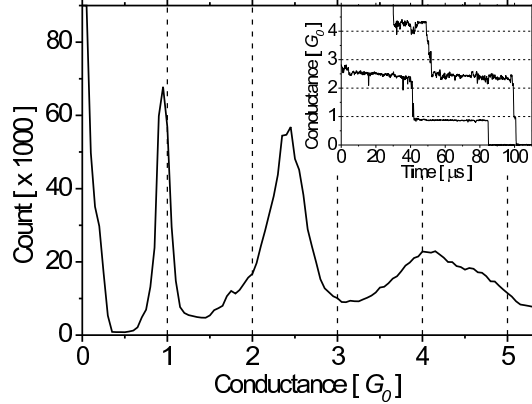


FIG. 3: Global histogram of conductance from Ag NWs. The main features are the peaks located at $1 G_0$, $2.4 G_0$ and $4 G_0$. Inset: Typical conductance curves; note the plateaus connected by abrupt jumps.

presented in Fig. 2. Based on the experimental data, it is clear that a proper theoretical description should take into account the atomic arrangement of the NW. For this purpose we have used an approach introduced by Emberly and Kirczenow [24] that is based on the Extended-Hückel-Theory, the latter being employed to obtain the molecular orbitals (MO) of the Ag NWs [25]. The MO calculations take into account the s, p and d orbitals of the Ag atoms in the NW, as well as overlap and energy matrix elements extending beyond the first neighbor atoms. The electronic transport was described within the Landauer scattering formalism [1]. A whole description of the procedure has been presented elsewhere [26]. Fig. 4 shows theoretical calculations of the conductance for the different NW morphologies observed in the HRTEM images. The experimental results are to be compared with the conductance at the Fermi energy (E_F), which is indicated by the vertical line in the figure. The conductance curve oscillations in Fig. 4 are sensitive to the atomic positions, therefore an average of the conductance around E_F yields a more representative value of G that takes into account the atomic vibrations during the measurement.

The calculations show that [100] Ag ATCs (interatomic distance 0.29 nm) display the expected conductance close to the quantum G_0 (Fig. 4a) [7, 8]. The 1/1 rod, composed of two parallel atom chains, shows a conductance close to $1.8 G_0$ (Fig. 4b), however, the Ag global histogram (Fig. 3) does not show a peak associated with this value and it must be concluded that this atomic arrangement does not occur in our experiments. As for the 2/1 [110] NW the model predicts a conductance at $G(E_F) \sim 2.5 G_0$ that is in remarkable agreement with

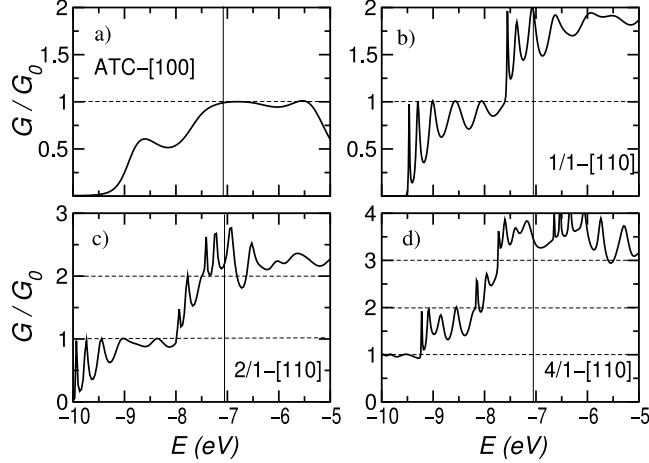


FIG. 4: Theoretical calculations of the quantum conductance G as a function of the electron energy for different Ag NW morphologies: 2 atoms long ATC in the $[100]$ direction; 1/1 (b), 2/1 (c) and 4/1 (d) rod-like structures along the $[110]$ direction. The conductance is plotted in units of G_0 and the vertical line indicates the Fermi energy.

the main peak of the conductance histogram. These results show that the 2/1 structure is in fact the minimal rod-like silver NW (Fig. 2e). Finally, the conductance calculation for the 4/1 rod with rectangular cross section yields $G(E_F) \sim 3.8 G_0$, which should be associated with the observed conductance peak at $\sim 4 G_0$. All the theoretical conductance values show an excellent agreement with the experiments, confirming the proposed correlation between HRTEM images and conductance histogram.

In summary, we have been able to reveal the preferred structures of silver NWs generated by mechanical elongation and determine the conductance for each kind of NW. This correlation between structural and electronic properties was confirmed by means of theoretical calculations. These results represent a clear evidence of the need to determine precisely the atomic arrangement of NWs in order to analyze in detail their conductance behavior. Although the surface properties of silver suggested that Ag NWs should be quite different from gold ones, the 4/1 or 2/1 rod-like wire would have been rather difficult to predict. This fact emphasizes the importance of experiments allowing the direct determination of atomic arrangements in the field of nanosystems.

The authors are grateful to FAPESP, CNPq, and LNILS for financial support

* Electronic address: ugarte@lnls.br

- [1] J.M. van Ruitenbeek in *Metal Clusters at Surfaces*, edited by K.-H. Meiwes-Broer, Cluster Series (Springer-Verlag Berlin Heidelberg, New York, 2000).
- [2] L. Olesen, *et al.*, Phys. Rev. Lett. **72**, 2251 (1994).
- [3] J.M. Krans *et al.*, Nature **375**, 767 (1995).
- [4] J.M. Krans *et al.*, Phys. Rev. Lett. **74**, 2146 (1995).
- [5] U. Landman *et al.*, Science **248**, 454 (1990).
- [6] G. Rubio, N Agrait and S. Vieira, Phys. Rev. Lett. **76**, 2302 (1996).
- [7] H. Ohnishi, Y. Kondo, and K. Takayanagi, Nature **395**, 780 (1998).
- [8] V. Rodrigues, T. Fuhrer and D. Ugarte, Phys. Rev. Lett. **85**, 4124 (2000).
- [9] L.D. Marks, Rep. Progr. Phys. **57**, 603 (1994).
- [10] S.M. Foiles, M.I. Baskes, M.S. Daw, Phys. Rev. B **33**, 7983 (1986).
- [11] J.L. Costa-Krämer *et al.* in *Nanowire*, edited by P.A. Serena and N. García, NATO ASI Series E: Applied Science, Vol. **340** (Kluwer Academic Publishers, The Netherlands, 1997).
- [12] Y. Kondo and K. Takayanagi, Phys. Rev. Lett. **79**, 3455 (1997).
- [13] V. Rodrigues and D. Ugarte, Europ. J. Phys. D **16**, 395 (2001).
- [14] D.B. Williams and C.B. Carter, *Transmission Electron Microscopy* (Plenum Press, New York, 1996) p. 465.
- [15] Y. Takai *et al.*, Phys. Rev. Lett. **87**, 106105 (2001).
- [16] Y. Kondo and K. Takayanagi, Science **289**, 606 (2000).
- [17] V. Rodrigues and D. Ugarte, Phys. Rev. B. **63**, 073405 (2001).
- [18] V. Rodrigues and D. Ugarte, submitted.
- [19] C.J. Muller, J.M. van Ruitenbeek and L.J. de Jongh, Phys. Rev. Lett. **69**, 140 (1992).
- [20] V. Rodrigues, Master thesis, Universidade Estadual de Campinas, 1999; V. Rodrigues and D. Ugarte, Rev. Sci. Instrum., submitted.
- [21] A.I. Yanson *et al.*, Nature **395**, 783 (1998).
- [22] B.D. Hall, M. Flüeli, R. Monot and J.-P. Borel, Phys. Rev. B. **43**, 3906 (1991).
- [23] B.H. Hong *et al.*, Science **294**, 348 (2001).
- [24] E.G. Emberly and G. Kirczenow, Phys. Rev. B **58**, 10911 (1998); *ibidem* **60**, 6028 (1999).

- [25] J.P. Lowe, *Quantum Chemistry* (Academic, NY, 1978). For a numerical implementation of the method: G.A. Landrum and W.V. Glassy, YAeHMOP project, <http://yaehmop.sourceforge.net>.
- [26] L.G.C. Rego *et al.*, in preparation.